

## Fundamentals of Vision

Antonio Guirao<sup>\*,†</sup>, David R. Williams<sup>\*,‡</sup>, Jason Porter<sup>\*,‡</sup>, and Yasuki Yamauchi<sup>\*</sup>

<sup>\*</sup> *Center for Visual Science, University of Rochester, Rochester, New York, 14627, USA*

<sup>†</sup> *Laboratorio de Optica, Universidad de Murcia, Campus de Espinardo (Edificio C), 30071 Murcia, SPAIN*

<sup>‡</sup> *The Institute of Optics, University of Rochester, Rochester, New York, 14627, USA*

### 1. Introduction

Though it is well established that the human eye suffers from more monochromatic aberrations other than defocus and astigmatism, there has been relatively little work on correcting them. However, recent advances in the measurement of these aberrations and their compensation with adaptive optics has made it possible to provide the eye with unprecedented optical quality. An observer viewing the world through adaptive optics will see a sharper image of it than they have ever seen before. Adaptive optics can correct the aberrations for light leaving the eye as well as for light entering it, which make it possible to obtain sharper images of the living retina as well.

The eye is not the only element responsible for vision. The retina and the visual cortex are also involved in the visual process. While the eye's optics can be improved by correcting the aberrations, there are further limits imposed by retinal and neural factors. We begin this chapter with a review of what is known about the functional anatomy of the eye, the retina and the visual cortex. This aims to provide an insight into the different factors limiting human vision. Moreover, we try to provide an understanding of how to improve the eye's optics as well as what benefits can be obtained from retinal imaging. Finally, we discuss more in detail the limits imposed by the retinal and neural factors.

### 2. Functional Anatomy of the Eye and Brain

Visual perception results from a series of transformations that can be classified in three stages: optical, retinal, and cortical. A more detailed review of these stages can be found in the bibliography (Wandell, 1995; Rodieck, 1998; Palmer, 1999). The light arriving at the eye from a scene is first focused by the eye's optics to form an image on the retina. This image is then transformed into neural signals by the photoreceptors. These signals exit the eye via the optic nerve and are transformed into cortical representations in the brain.

## 2.1. Optical processing

The eyes sit in their sockets, which protect them yet allow them to rotate. Each eye is moved by the coordinated use of six small muscles, called the extraocular muscles. Small, rapid eye movements (saccades) are necessary for scanning different regions of the visual field.

The eyes have two important optical functions that are also shared with cameras: to gather light reflected from surfaces in the world, and to focus this light to form a clear image on the back of the eye. If the image is not clearly focused, fine-grained optical information will be lost, deteriorating our spatial vision.

There are several parts of the eye that accomplish different optical functions (Chapman, 1995). The first component, shown in Fig. 1, is the cornea which is a thin, transparent medium on the front of the eye. The cornea separates

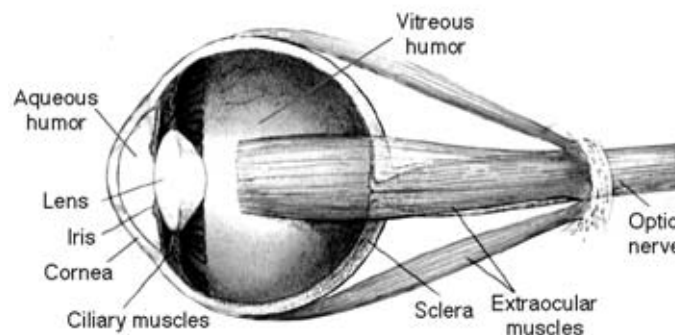


Figure 1. The human eye. (Hubel, 1988)

the outside air from the aqueous humor, a liquid that fills the cavity behind the cornea. Next is the pupil, a variably sized opening in the opaque iris, which gives the eye its external color. Behind the iris is the crystalline lens. The ciliary muscles are attached to the edge of the lens and control its shape. Following the lens is a liquid filled chamber containing the vitreous humor. Finally, the multi-layered retina is at the back of the eye. It is here where the light is absorbed by the photoreceptors and is transformed into neural impulses which exit through the optic nerve.

Each of the aforementioned components perform a critical role. The amount of light reaching the retina is regulated by the iris and the pupil. The pupil dilates to permit more light to enter the eye in low illumination conditions, and constricts under high illumination conditions. The diameter of the pupil can vary between 2 and 8 mm, allowing for a 16-fold increase or reduction in light intensity at the retina. The cornea and the crystalline lens are responsible for refracting the light entering the eye to produce a focused image on the retina. Two-thirds of the total refraction of the light propagating through the eye occurs at the air interface of the cornea. The lens is particularly important in accomplishing the task of accommodation because of its ability to change shape. The curvature of the lens may be increased when the ciliary muscles contract, thereby increasing

the refractive power of the eye and allowing near objects to come into focus on the retina.

The length of the eye is approximately 25 mm and its focal length is approximately 17 mm. If the image of a distant object is focused on the retina when the ciliary muscles are relaxed, the eye is said to be emmetropic. If the power of the eye is either too large or too small in comparison with the length of the eye, people are said to be nearsighted (myopic) or farsighted (hyperopic), respectively. The ability of the eye to accommodate decreases with age, a condition known as presbyopia.

The optics of the eye therefore impose the first limit to vision. In the eye there are three sources of retinal image blur: diffraction, aberrations, and scattering. Scattering appears because of non-homogeneities within the ocular media, such as the aqueous or vitreous humors and the lens. Scatter and absorption of light by the ocular media increases with age (Owsley & Sloane, 1990). However, at least in young normal eyes, scattering is a minor factor. Diffraction is the dominant source of image blur for small pupils (up to 3 mm). For large pupils, aberrations become the dominant source, overwhelming the effects of diffraction. It is well known that normal eyes suffer from higher order aberrations, in addition to defocus and astigmatism, that further degrade the retinal image (Howland & Howland, 1977; Walsh & Charman, 1985; Liang & Williams, 1997). The aberrations also tend to increase with age (Guirao *et al.*, 1999).

## 2.2. Retinal processing

Following the eye's optics, the next stage of image processing occurs at the retina. The retina is a neural circuit that contains many blood vessels and millions of connected cells, most about 1 to 5 microns in diameter. The retinal thickness varies from a maximum of 0.5 mm to a minimum of 0.2 mm at the fovea, the region of best acuity and color vision. The healthy human retina, shown in Fig. 2, has five layers of densely packed, well-organized tissues. The cell bodies of the neurons are grouped into three layers, each separated by a layer containing the contacts (or synapses) between neurons. There are five main types of cells in the retina. Of these, the photoreceptors (cones and rods) are the only ones sensitive to light and are responsible for its detection. Light must first pass through the first four layers of the retina in order to reach the photoreceptors, which lie in the outermost portion of the retina. Photoreceptors have two main components: the inner and outer segments. The inner segments guide light to the photopigments contained in the outer segments.

Other retinal cells include the horizontal, bipolar, amacrine, and ganglion cells, which integrate responses from the nearby cells. Photoreceptors make contact with bipolar and horizontal cells. Amacrine cells make connections with bipolar cells, ganglion cells and other amacrine cells. The ganglion cells are only connected with bipolar and amacrine cells, so the simplest visual pathway to the brain is from the photoreceptors to the bipolar cells which feed into the ganglion cells. The ganglion cells provide the only retinal output signal. Their terminals converge at the optic nerve, and they exit the retina at a single location called the optic disk. There are no photoreceptors in the optic disk. For this reason, the optic disk is also called the "blind spot".

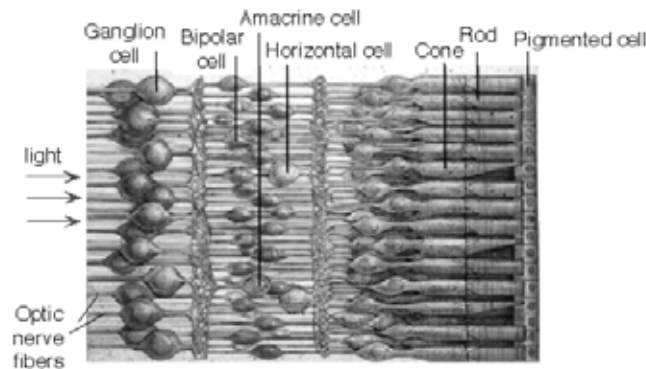


Figure 2. Transverse section of the multi-layered human retina. (Hubel, 1988)

Fig. 3 shows the two classes of photoreceptors in the retina: rods and cones. Rods are typically longer than cones and have cylindrical outer segments, whereas cones are shorter and thicker, and have cone-shaped outer segments. Rods are more numerous, about 100 million per eye, and are located everywhere in the retina except at its very center (fovea). They are used exclusively for vision at very low (scotopic) light levels and are very sensitive detectors. Cones are less abundant (only about 5 million per eye), are much less sensitive to light, and are concentrated in the fovea. The size and separation between adjacent cones increases as one moves from the fovea to peripheral retina where the cones become much larger than the rods and are widely separated (Fig. 4). Cones are responsible for vision under most normal (photopic) lighting conditions and for color vision. There are three types of cones (L, M, and S-cones), each one maximally sensitive to a different wavelength. The central, rod-free portion of the fovea subtends a visual angle of slightly less than 2 degrees. (For comparison, the moon subtends half a degree of visual angle while your thumb held at arm's length subtends one and a half degrees of visual angle). Both color and spatial vision are most acute in the fovea.

Photoreceptors have interesting optical properties, acting like optical fibers that guide light towards the outer segment. There, the photon energy is converted into a neural signal. The outer segment contains billions of light-sensitive pigment molecules. The pigment found in rods is called rhodopsin. When a photon is absorbed by a rhodopsin molecule (called bleaching), the molecule isomerizes, which ultimately alters the flow of current into the cell. The electrical changes that result from many photons being absorbed within the same photoreceptor are integrated in the response. When a pigment molecule is bleached, its color changes and it becomes transparent, unable to absorb another photon until the molecules are restored to their original unbleached state by the ongoing process of pigment regeneration.

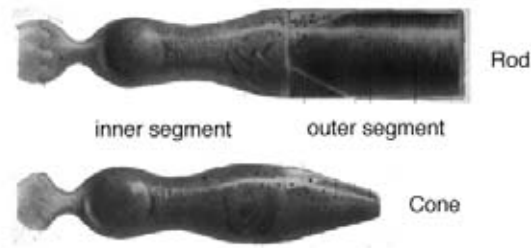


Figure 3. Cross-section of rod and cone photoreceptors (Schnapf & Baylor, 1987).

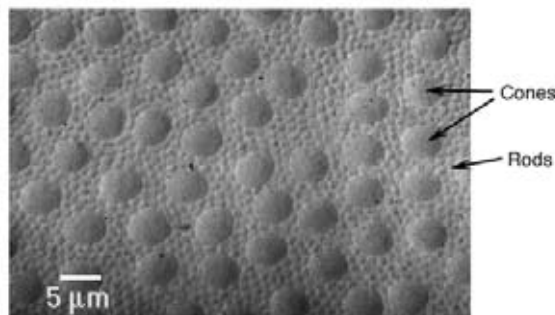


Figure 4. Image of the mosaic of photoreceptors obtained with a microscope from peripheral retina (Packer, ?).

### 2.3. Cortical processing

As shown in Fig. 5, neural impulses leave the retina via the optic nerve and travel to the optic chiasm. Here the nerve fibers from the nasal side of the fovea in each eye cross over to the opposite side of the brain, while the fibers receiving input from temporal retina remain on the same side of the brain. From the chiasm, there are two separate pathways into the brain on each side. The larger pathway first goes to the lateral geniculate nucleus (LGN) of the thalamus and then to a large area in the occipital cortex, called primary visual cortex, or area V1, that consists of approximately 150 million neurons. More than 20 other cortical areas in addition to V1 have been found to play a significant role in visual perception. The LGN is a three-dimensional structure that receives input from both eyes. The LGN is laminar and each of its layers gets signals from only one eye alternatively. Each layer is laid out spatially like the retina of the eye from which it receives input. This is called retinotopic mapping or topographic mapping because it preserves qualitative spatial relations between the retina and the LGN. However, this transformation distorts quantitative relations: the central area of the visual field receives proportionally much greater representation in the

cortex than the periphery does. This is called the cortical magnification factor. It reflects the fact that we have more detailed spatial information about objects in the central region of the retina than that about those in peripheral regions.

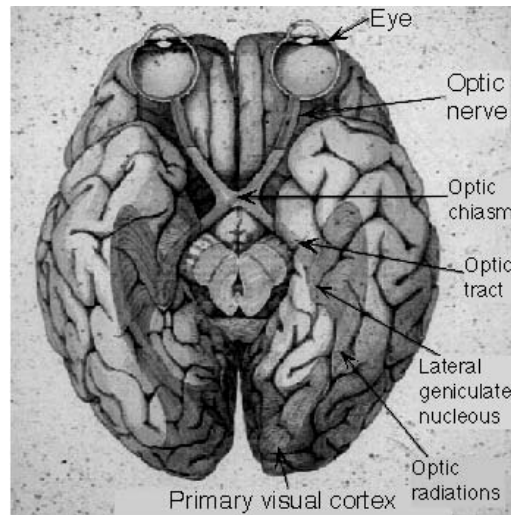


Figure 5. Cross-section of the brain (Hubel, 1988).

### 3. Role of Adaptive Optics: To Improve Vision and Retinal Imaging

Why improve the optics of the eye? First, adaptive optics is a tool that can be used to explore the viability of improving vision, shown in Fig. 6(a) (Williams *et al.*, 2000; Miller, 2000). As pointed out above, the eye's aberrations impose the first limit on degrading spatial vision. Retinal and neural factors are unavoidable, unlike aberrations, which can be corrected. To date, spectacles or contact lenses have corrected only spherical and cylindrical errors (defocus and astigmatism) of the eye. The first spectacles were developed 7 centuries ago and used positive lenses to magnify the image in farsighted individuals (hyperopes). The first spectacles used to correct myopia originated in the 16th century. Spectacles having the ability to correct astigmatism as well as defocus were not introduced until 150 years ago. However, recent experiments with adaptive optics, using a deformable mirror to correct the eye's aberrations, have shown that spatial vision can be improved if higher order aberrations besides defocus and astigmatism are corrected in the eye (Liang *et al.*, 1997). These results encourage implementing new methods of correction, such as customized contact lenses and intraocular lenses, or customized laser refractive surgical procedures to also eliminate the eye's higher order aberrations. The implications of a customized correction of the eye's optics on visual performance will be discussed in the next two chapters.

A second application of adaptive optics in vision is to increase the contrast and resolution of images of the retina (Fig. 6(b)). This issue is discussed next.

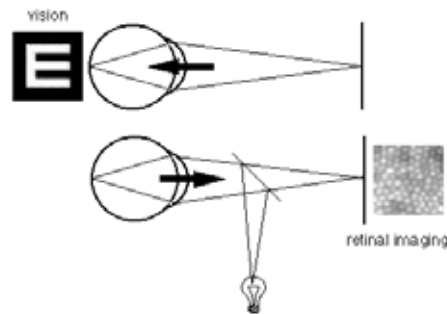


Figure 6. Adaptive optics can (a) improve vision and (b) retinal imaging by correcting the eye's higher order aberrations.

#### 4. Fundus Imaging as a Diagnostic Tool

The interior of the eye can be viewed with the aid of a simple optical device called an ophthalmoscope. When light strikes the retina, a portion is reflected back and leaves the eye. This exiting light can provide a view of the back of the eye, or a fundus image. At first thought, retinal imaging may seem to be a simple task given the transparency and accessibility of the eye in comparison with imaging internal organs, such as the heart. The main applications of retinal imaging include characterizing the basic anatomy and physiology of the retina, understanding vision changes caused by age or disease, discovering disease mechanisms, and providing care for patients with diseases.

For clinical specialists, viewing the fundus is the most useful diagnosis tool. For some diagnostic purposes, the neural retina itself is of interest; for others, the blood vessels or structures behind the retina are of interest. There are many ways in which retinal function may be impaired as a result of disease. One of the most common diseases is glaucoma, which results from an increase in the pressure within the eye that damages nerve fibers leaving the optic nerve. Other diseases include diabetes, which damages small blood vessels, or retinitis pigmentosa, in which photoreceptors degenerate allowing the photopigments to leak and disperse in the retina. A fundus camera can show the presence of retinitis pigmentosa, as depicted in Fig. 7.

Optical techniques used for retinal imaging can non-invasively provide a high resolution image of living structures in the eye on the order of microns in size. For example, angiograms image retinal capillaries and vessels to detect diabetes. Scanning laser polarimetry is used to diagnose glaucoma and optic nerve diseases. Confocal imaging offers a cross-sectional map of the retina.

Although certain types of pathological structures are visible with these conventional methods, the microscopic structure of the retina is not visible with conventional imaging techniques. The aberrations inherent in the optics of the eye are sufficiently large to limit retinal image quality. During the last ten years, different research groups have developed high-resolution retinal cameras that address these imaging problems (Roorda *et al.*, 1997; Wade & Fitzke, 1998; Miller *et al.*, 1996; Marcos *et al.*, 1996; Artal & Navarro, 1989). The designs

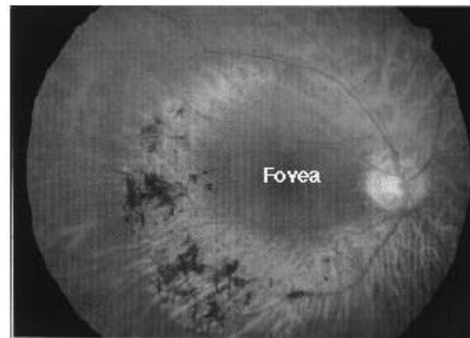


Figure 7. Image of an eye with retinitis pigmentosa taken using a conventional fundus camera (Rodieck, 1998). The optic disk, fovea, neural fibers, and blood vessels are all visible in this image. The dark shadows are areas where photopigment has leaked out of the degenerating photoreceptors.

incorporate such methods as dilating the pupil, using quasi-monochromatic illumination for imaging with short exposure times of a few milliseconds, and precisely correcting the eye's defocus and astigmatism. These retinal images, containing in some cases spatial frequencies well above 60 c/deg, have given a first view of single cells in the retina of the living human eye. However, the microscopic structure revealed in the images has been of low contrast and limited to subjects with good optics. To achieve better imaging will require the correction of aberrations beyond defocus and astigmatism. Adaptive optics can correct the aberrations introduced by the eye and improve image contrast, revealing fine structures in the retina. Adaptive optics may provide the resolution of microscopy in *living* tissues.

Similar to astronomers, who use adaptive optics to observe and resolve fine details in the sky, vision scientists can use adaptive optics to resolve fine details in the fundus of the eye and may be able to better diagnose and treat pathologies or better understand the physiology of the retina.

## 5. Measures of Visual Performance

A number of different methods may be used to measure the visual performance of the eye. Here, we will explain the contrast sensitivity function and several other methods used to measure visual acuity.

### 5.1. Visual acuity and visual acuity charts

Visual acuity refers to the concept of sharpness of vision. However, multiple definitions are necessary to cover the wide range of visual tasks that we encounter in our daily lives (Smith & Atchison, 1997; Michaels, 1985). Thus, when asked for a definition of acuity, the psychophysicist speaks of contrast threshold limits, the physiologist of receptive fields, the optical engineer of modulation transfer functions, the psychologist of form perception, and the ophthalmologist recites Snellen fractions.

For our purposes, visual acuity is quantified in terms of the finest size of detail in a scene that can just be resolved by the eye. The greatest visual acuity of the human eye is at the fovea and decreases rapidly with distance (or eccentricity) from the fovea.

Different targets can be used such as lines, bars, grating, and letters (Bailey & Lovie, 1976).

- *Grating acuity*

Periodic gratings of equally spaced black and white bars can be used to measure visual acuity. They may have square or sinusoidal forms. Grating acuity is the highest grating frequency that can be resolved by the eye. A typical acuity in a normal human eye ranges from 30 to 60 c/deg at optimum luminances.

- *Point source acuity*

Point source acuity is a measure of the ability to resolve two very close point sources. The resolution depends upon whether the sources are white on a black background or black on a white background. For white sources against a dark background the resolution within an individual is about the same as the subject's grating acuity. In a normal eye, two sources can be separately distinguished if their separation is greater than about 0.5 to 1 minute of arc.

- *Snellen acuity and Snellen chart*



Figure 8. The Snellen chart consists of rows of letters of the alphabet, printed with maximum contrast, with letters in each row having a different size and corresponding to a different level of acuity.

Clinical visual acuity is usually defined as a letter acuity, using a standard letter chart (shown in Fig. 8) observed at a fixed distance. The size of the smallest letters that can be recognized is taken as the clinical visual acuity of the subject.

The best known and most widely used system of acuity notation is the Snellen fraction, V:  $V=d/D$ , where d is the distance at which a given

letter can just be discriminated and  $D$  is the distance at which the same letter subtends 5 minutes of arc. The reading distance is usually 6 meters (20 ft). At this distance, the letter size corresponding to 20/20 (6/6 in meters) vision is 5 minutes of arc in height. Acuity of 20/200 means that the subject can read at 20 ft a letter that subtends 5 minutes at 200 ft; i.e., the smallest letter that this subject can read at 6 m subtends 50 minutes. A subject with 20/10 vision could read a letter at 6 m that subtends 2.5 minutes of arc.

The 20/20 level letter E may be regarded as being composed in the vertical dimension of three horizontal black lines separated by two horizontal white lines having the same spacing as a grating with a spatial frequency of approximately 0.5 c/min, or 30 c/deg. Hence, the typical acuity limit of 5 minutes of arc of letter height is equivalent to about 30 c/deg grating acuity (20/20). A subject with 20/40 vision can reach a grating acuity of 15 c/deg. However, assigning equivalent periodic frequencies to non-periodic targets should be done with some caution. A 20/10 letter has the same stroke periodicity as a 60 c/deg grating. One may ask why the average Snellen acuity is not 20/10 if the maximum human grating acuity is approximately 60 c/deg? Grating targets usually extend over a larger visual angle than their equivalent Snellen letters which increases their visibility. The detection of gratings is a very different task than the recognition of Snellen letters. In Snellen acuity, the subject can be influenced by literacy and past experience. Letters present low spatial frequency cues due to the symmetry or asymmetry in the form that can help recognizing them. All of these factors make the comparison between Snellen and grating acuity problematic.

- *Vernier acuity*

Letter acuity is a good guide to reading performance but should not be used to predict visual performance for all other tasks, for example when reading scales or verniers. In these cases, a good judgement of the alignment of two lines or edges is required. The angular threshold for determining when two bars or edges are misaligned is called vernier acuity and is about 5 seconds of arc (or about 1/6 of the densest spacing of photoreceptors in the fovea, which is approximately 30 seconds of arc). Fig. 9 shows an example of the vernier acuity chart. The larger the offset, the easier the detection of the misalignment.

## 5.2. Contrast sensitivity function

The contrast sensitivity function (CSF) is the standard measurement of how sensitive observers are to gratings of different spatial frequencies. The CSF is determined by finding the threshold contrast at which the subject can detect a sinusoidal grating at each of a number of spatial frequencies. The reciprocal of the threshold is defined as the contrast sensitivity. At high spatial frequencies, the CSF monotonically decreases with spatial frequency, which means that the subject needs higher contrast to detect finer details. It is determined by finding the lowest threshold contrast at which an observer can just barely detect a sinusoidal grating at a number of spatial frequencies (Campbell & Green, 1965).

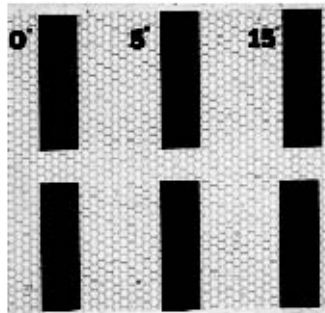


Figure 9. Vernier acuity chart with bars that are off-set by 0, 5 and 15 seconds of arc.

The fastest and easiest procedure for measuring contrast thresholds is using the method of adjustment. The subject adjusts a knob that controls the contrast of a grating of a particular spatial frequency on a CRT until they can just detect it. This adjustment is repeated for several gratings of different spatial frequencies. The results of such an experiment can be summarized by plotting the subject's contrast sensitivity as a function of spatial frequency (Fig. 10). Threshold is high when sensitivity is low and vice versa.

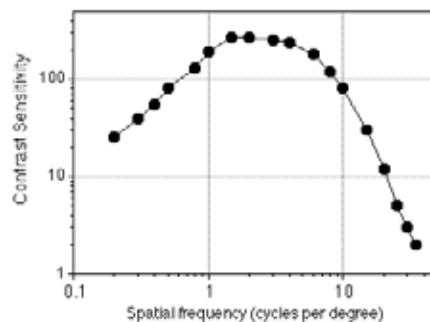


Figure 10. Contrast sensitivity function obtained experimentally from the measurement of a subject's sensitivity to gratings of different spatial frequencies.

The visual system acts as a band-pass filter and is most sensitive to intermediate spatial frequencies at about 4 to 5 c/deg. Moreover, the sensitivity decreases dramatically under low-light (scotopic) conditions. Therefore, at night, when primarily the rods are operating, human vision lacks the high acuity that it has in daylight conditions. This is mainly due to the fact that rods are very broadly dispersed in the fovea, the region of highest visual acuity. Their density increases dramatically as one moves further into the periphery, where visual acuity becomes poorer.

Visual performance varies across different species. The maximum spatial frequency that the human eye can perceive is about 60 c/deg, whereas the cat and the housefly can only perceive spatial frequencies of up to 5 and 0.5 c/deg, respectively. Although resolution generally increases linearly with the eye's size, the maximum resolution of an eagle (150 c/deg) is 2.5 fold larger than that of a human, probably due to the facts that eagles possess a more densely packed photoreceptor mosaic and have superior optical quality. Neural factors, such as photoreceptor spacing (see the next section), and optical factors both limit visual performance. While neural limitations on vision cannot be avoided, the optics of the eye may be corrected and improved.

## 6. Sampling and Aliasing

In this section, we consider how the photoreceptor mosaic encodes high-spatial-frequency patterns. Since the mosaic contains a discrete number of photoreceptors, the retinal image is detected (or sampled) only at the points that have a receptor. If the spacing between photoreceptors is too large, the image will not be adequately sampled and important information in the original image can be lost. This situation is analogous to the detection of an input signal by a CCD camera, which contains a discrete number of pixels. The value of the signal (retinal image) at each of the sampling points is the sampled value, the interval that separates the sampling points (separation between photoreceptors) is the sampling interval and the reciprocal of the sampling interval is the sampling frequency.

The term used to describe errors due to sampling is aliasing, as sampling causes high spatial frequencies in the image to masquerade or alias as low spatial frequencies. Fig. 11(a) shows this effect for a one-dimensional array of photoreceptors that is sampling two sinusoidal gratings with different spatial frequencies. Notice that the light intensity is identical at each of the sample locations. The cone mosaic is blind to the fact that the retinal images differ between the sample locations defined by the photoreceptors. Since the photoreceptor mosaic does not retain any information that these two images are in fact different, the brain cannot distinguish them. The brain interprets the pattern as the low frequency regardless of the actual spatial frequency presented. Fig. 11(b) shows aliasing for an array of sample locations taken from an image of the human cone mosaic. When the fundamental spatial frequency of a grating is low, the mosaic has an adequate number of samples to represent it. However, when the spatial frequency is high, a low frequency pattern emerges. The irregularity of the low frequency alias is a result of the disorder in the cone mosaic.

A critical question then arises: what is the optimum sampling frequency that is required to produce the best possible image on the retina? In other words, what is the maximum spatial frequency in a signal that can be adequately represented for a fixed sampling interval?

### 6.1. The sampling theorem

A finite energy function  $f(x)$  having a band-limited Fourier transform, can be completely reconstructed from its  $n$  sampled values,  $f(n\Delta)$ , where  $\Delta$  is the

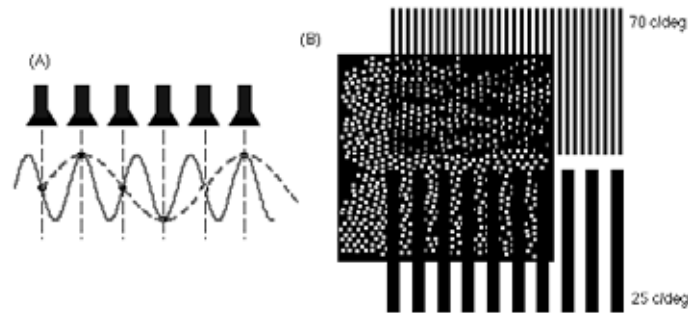


Figure 11. (a) Two sinusoidal stimuli sampled by an array of cones. The spatial frequency of one stimulus (solid line) is three times the frequency of the other (dashed line). The cone response interprets the high-frequency pattern as a low-frequency pattern (aliasing), as shown by the location of the dots. (b) Two square-wave patterns are seen through a sampling array resembling the cone mosaic. After sampling, the high-frequency pattern appears as a distorted, low-frequency signal.

sampling interval and  $f_s = 1/\Delta$  is the sampling frequency, by the expression:

$$f(x) = \sum_{n=-\infty}^{\infty} f(n\Delta) \cdot \text{sinc}(\pi(x/\Delta - n))$$

provided that  $f_s \geq 2f_N$ , where  $f_N$  is the cutoff frequency of the Fourier transform or Nyquist frequency (Goodman, 1996). In other words, the function can be recovered from the sampled values if the sampling frequency is larger than twice the Nyquist frequency. If the sampling frequency does not exceed this value, the recovered signal will be distorted. This phenomenon is known as aliasing.

Thus, for the eye, if the regular photoreceptor mosaic is allowed to sample spatial frequencies that are higher than the Nyquist limit (half the reciprocal of the spacing between adjacent receptors), the pattern produced by these frequencies is indistinguishable from a pattern containing a low spatial frequency. The resulting image looks like a low-frequency moiré pattern with the original image being distorted, as shown in Fig. 11(b). These patterns are sometimes seen on conventional television screens when patterns such as pin stripes on suits are displayed. In this case, the fundamental frequency of the pin stripe exceeds the highest frequency that can be adequately represented by the array of pixels on the screen. The critical limit above which aliasing occurs, or the Nyquist frequency, is  $f_N = 1/2\Delta$  (c/deg), where  $\Delta$  is the center to center spacing of adjacent photoreceptors in degrees of visual angle. In normal conditions of foveal vision, the L- and M-cones have the smallest spacing and limit the range of spatial frequencies that the eye can recover from an image. Anatomical and psychophysical estimates yield a typical spacing of human foveal cones of about 0.5 minutes of arc, which makes the Nyquist limit about 60 c/deg. This means

that any pattern containing spatial frequencies above 60 c/deg will be distorted by aliasing.

Even though the effects of aliasing have been observed and documented for some time, it was not until recently that the underlying mechanisms responsible for aliasing and the perception of moiré patterns were discovered. Helmholtz (1862) noted that fine parallel wires appeared wavy and distorted when viewed against a bright background. He attributed this distortion to the photoreceptor mosaic (Fig. 12). However, the range of spatial frequencies at which the effect became apparent (23-25 c/deg) were below the foveal Nyquist limit and, therefore too low to produce aliasing in the fovea. Byram (1944) produced high contrast retinal interference fringes by viewing a line source through a double slit diaphragm. He claimed that 86 c/deg fringes have a “definite wavy appearance and are subject to a rapid shimmering of fluttering movement”, attributing this effect to the cone mosaic. Campbell and Green (1965), using fringes generated with a laser interferometer also saw these effects. More recent experiments based on interferometry later demonstrated that the origin of the moiré patterns is due to aliasing by the cone mosaic (Williams, 1985b).

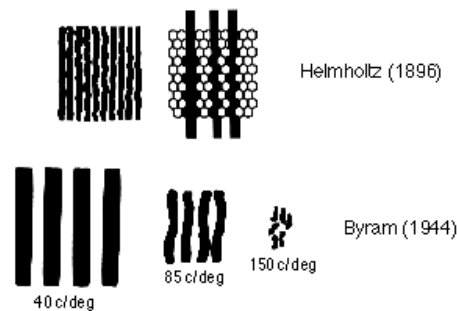


Figure 12. Helmholtz’s drawing of the observed fine patterns (top left), and his explanation in terms of cone sampling (top right). Byram’s drawings of interference patterns at three spatial frequencies, also demonstrating the effects of aliasing for spatial frequencies higher than the Nyquist limit of 60 c/deg.

## 6.2. L- and M-cones spacing and aliasing in foveal vision

To measure the sampling density of the mosaic formed by the L- and M-cones together, Williams (1985a) used a laser interferometer to produce high frequency, high contrast interference fringes onto the retina (see Fig. 13). The interference fringes imaged on the retina completely bypassed the optics of the eye and were not degraded by the eye’s aberrations. This method allowed for the measurement of the contrast sensitivity function at spatial frequencies above the resolution limit set by the eye under normal viewing conditions. These experiments were an objective demonstration of the aliasing phenomenon observed in human foveal vision, clarifying the constraints imposed by the photoreceptor mosaic on visual resolution.

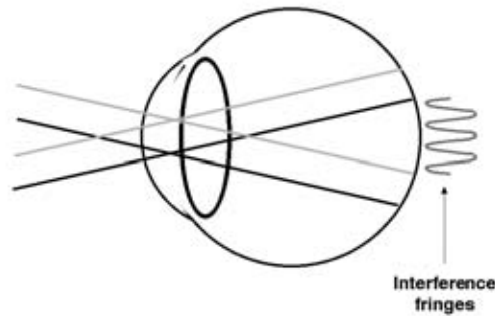


Figure 13. Two coherent light beams form interference fringes, unaffected by the eye's optics, on the retina. The spatial frequency of the interference fringe is proportional to the separation of the point sources in the entrance pupil. The contrast is modified by the time that the pairs of light beams overlap.

In this study, gratings with spatial frequencies over 200 c/deg were imaged on the retina at essentially unity contrast. Observers reported that interference fringes with spatial frequencies higher than the Nyquist limit of 60 c/deg appeared similar to those reported by Byram (1944), and Campbell & Green (1965). In the range between 0 and 45 c/deg, interference fringes can be seen across the central foveal region. As the spatial frequency increases above 45 c/deg, stripes can be seen only in a progressively smaller region of the visual field. At about 60 c/deg, the fine, regular bars are lost, and most observers reported the appearance of an annulus of fine wavy lines (see Fig. 14). The annulus corresponds to aliasing by cones just outside the foveal center, which are more widely spaced and alias at a lower spatial frequency than in the foveal center. As the spatial frequency increases, this annulus finally collapses to a circular patch at a frequency of 90-100 c/deg. Observers described this patch as resembling a fingerprint or pattern of zebra stripes. Between 100 and 150 c/deg, the patch of zebra stripes diminishes in size and between 150 and 160 c/deg, the zebra stripe pattern disappears abruptly. The explanation for the zebra stripes is that they represent a moiré fringe pattern resulting from an undersampling of the image (aliasing) by the photoreceptor mosaic. Even if the eye's optics were completely corrected, one could never experience an increase in visual acuity above 60 c/deg due to the sampling constraints of the cone mosaic.

Moiré patterns have the lowest spatial frequency when the spacing of the elements in the two patterns producing the moiré is the same. Thus, the zebra stripe should have the lowest spatial frequency when the period of the interference fringe equals the spacing of rows of foveal cones. Williams (1985a, 1988) found this frequency to have an average value of 111 c/deg corresponding to an intercone spacing of 0.54 minutes of arc of visual angle (or 2.6 microns). This agrees quite well with the anatomical data for the spacing of the L- and M-cones at the foveal center (Curcio *et al.*, 1990). Since the moiré pattern is quite regular, the human fovea appears to have a regular lattice structure. Lattice quality

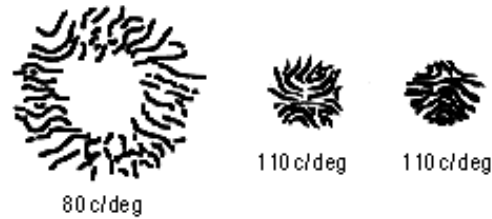


Figure 14. Drawings by two observers of the appearance of an 80 c/deg and an 110 c/deg interference fringe. Scale bar corresponds to 1 deg of visual angle (Williams, 1985a).

diminishes rapidly with retinal eccentricity because the rods begin to intrude and the cone spacing increases.

### 6.3. The spacing and aliasing of S-cones

The sampling distribution of the short-wavelength cones was the first to be measured empirically. Psychophysical experiments by Williams *et al.* (1981) took advantage of several features of the S-cones. The sensitivity of the S-cone photopigment is significantly higher than that of the L- and M-cones. As a result, if we present the visual system with a light containing only short-wavelengths, the S-cones will absorb more quanta than the other two classes. A second special feature of the S-cones is that they are relatively sparse in the retina and their number is quite small compared to the other two classes.

In the experiment by Williams *et al.* (1981), the subjects visually fixated on a small mark and a stimulus was presented. The subject indicated whether or not the stimulus was visible. If the short-wavelength test light fell upon a region that contained S-cones, sensitivity should have been relatively high. On the other hand, if that region of the retina contained no S-cones, sensitivity should have been rather low. Hence, from the spatial pattern of visual sensitivity, Williams *et al.* inferred the spacing of the S-cones in the fovea, as shown in Fig. 15. In the very center of the fovea, there is a large valley of low sensitivity. In this region, there appear to be no short-wavelength cones at all. From about half a degree from the center of the visual field, there is a small region of high sensitivity, indicating the presence of S-cones. Around the central fovea, the typical separation between the inferred S-cones is about 8 to 12 minutes of visual angle. Thus, there are 5 to 7 S-cones per degree of visual angle on the retina.

Anatomical measurements confirm these psychophysical results. DeMonasterio *et al.* (1985) applied a yellow, short-wavelength sensitive dye to the retina and then exposed the retina to a short-wavelength light source. The S-cones stimulated with short-wavelength light are the only ones that stain and change color (Fig. 16). In agreement with the psychophysical observations by Williams *et al.* (1981), DeMonasterio *et al.* found that S-cones are absent from the central fovea, having their peak density 1 degree from the central fovea, and are widely

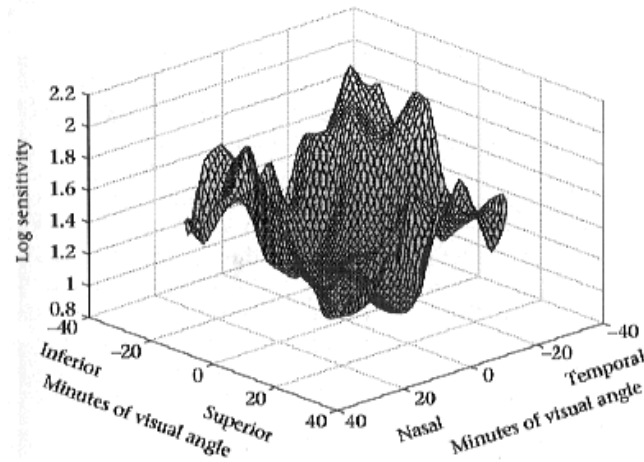


Figure 15. Threshold sensitivity to a short-wavelength test light presented on a yellow background. The local peaks in sensitivity correspond to the positions of the S-cones (Williams *et al.*, 1981).

spaced compared to the L- and M-cones. More recently, Curcio *et al.* (1991), used a biological marker specific to the S-cones to confirm the measurements of Williams *et al.* (1988) and showed that the average spacing between the S-cones is 10 minutes of arc.

Williams & Collier (1983) used the properties of sampling and aliasing to also confirm the spacing between S-cones. Short-wavelength sinusoidal patterns seen only by the S-cones appeared as low-frequency aliased patterns when the stimulus exceeded the Nyquist frequency of the S-cones of 3 c/deg.

Table 3 summarizes the spacings, densities and Nyquist frequencies for the three classes of cones in the fovea.

Table 3. The spacings, densities and Nyquist frequencies of cones

Cone class	Spacing		Density		Nyquist (c/deg)
	min. of arc	microns	cones/deg	cones/mm <sup>2</sup>	
M, L	0.51	2.5	111	~160,000	60
S	10	48	6	~450	3

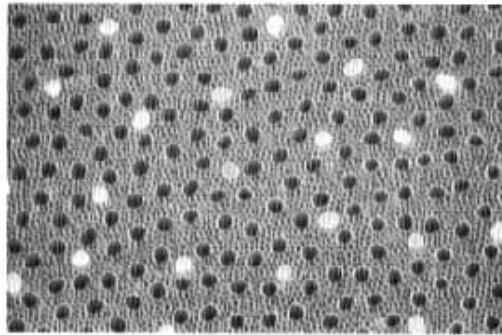


Figure 16. Cross-section of a Macaque retina. S-cone inner segments that absorbed a yellow dye appear as bright circles. The dark circles are the L- and M-cones. (DeMonasterio *et al.*, 1985).

#### 6.4. Post-receptoral factors: the neural CSF

The CSF of the visual system to interference fringes provides a lower best estimate of the contrast sensitivity of the retina and the brain alone (or neural contrast sensitivity), since interference fringes are immune to most sources of optical blurring in the eye. By using a laser interferometer Williams (1985a) showed that fringes can be resolved for spatial frequencies up to 60-70 c/deg. However, above these frequencies, observers can still detect the presence of fringes because of the moiré or zebra stripe patterns formed between the fringes on the cone mosaic, as explained before. An additional study (Williams, 1985b) further explored the neural sensitivity function in the range over which fringes can normally be resolved. Fig. 17 shows the average neural CSF obtained in comparison with the CSF for normal viewing conditions. These measurements indicate that the neural visual system is substantially more sensitive to spatial frequencies near the resolution limit than previously believed. Hence, the benefit of an improvement in the optics of the eye will be captured by the neural system.

#### References

- Artal, P. & Navarro, R., 1996, *Opt. Lett.*, 14, 1098.  
 Bailey, I. L. & Lovie, J. E., 1976, *Am. J. Optom. Physiol. Opt.*, 53, 740.  
 Byram G. M., 1944, *J. Opt. Soc. Am.*, 34, 718.  
 Campbell F. W. & Green D. G., 1965, *J. Physiol.*, 1981, 576.  
 Chapman, W. N., 1995, in *Optics of the Eye*. In: *Handbook of Optics* (2nd ed.). cap. 24, (McGraw-Hill, New York).  
 Curcio, C. A., Sloan, K. R., Kalina, R. R. & Hendrickson, A. E., 1990, *J. Comp. Neurol.*, 292, 497.  
 Curcio, C. A., Allen, K. A., Sloan, K. R., Lerea, C. L., Hurley, J. B., Klock, I. B. & Milam, A. H., 1991, *J. Comp. Neurol.*, 312, 610.

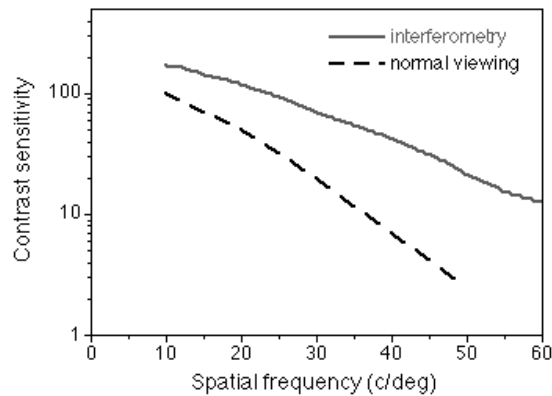


Figure 17. CSF measured with interferometry (the neural CSF) and the CSF for normal viewing conditions (representing the ocular and neural CSFs) for a pupil size of 3 mm. (Williams, 1985b).

- DeMonasterio, F., McCrane, E. P., Newlander, J. K. & Schein, S., 1985, *Inv. Ophth. Vis. Sci.*, 26, 289.
- Guirao, A., Gonzalez, C., Redondo, M., Geraghty, E., Norrby, S. & Artal, P., 1999, *Inv. Ophth. Vis. Sci.*, 40, 203.
- Goodman, J. W., 1996, *Introduction to Fourier Optics* (2nd ed.). (McGraw-Hill, New York).
- Helmholtz H., 1962, in *Helmholtz's treatise on physiological optics* (3rd ed.), Dover, New York.
- Howland, H. C. & Howland, B., 1977, *J. Opt. Soc. Am.*, 67, 1508.
- Hubel, D. H., 1977, *Eye, brain and vision*, (Scientific American library, New York)
- Liang, J. & Williams, D. R., 1997, *J. Opt. Soc. Am. A* 14, 2873.
- Liang, J., Williams, D. R. & Miller, D. T., 1997, *J. Opt. Soc. Am. A*, 14, 2884.
- Marcos, S., Navarro, R. & Artal, P., 1996, *J. Opt. Soc. Am.* 13, 897.
- Michaels, D. D., 1985, *Visual Optics and Refraction A clinical approach* (3rd ed.). Mosby Company, St. Louis.
- Miller, D. T., Williams, D. R., Morris, G. M. & Liang, J., 1996, *Vision Res.*, 36, 1067.
- Miller, D. T., 2000, *Physics Today*, January, 31.
- Packer, O., Hendrickson, A. E. & Curcio, C. A., 1989, *J. Comp. Neurol.*, 288, 165.
- Palmer, S. E., 1999, *Vision Science*. MIT Press, Cambridge.
- Rodieck, R. W., 1998, *The First Steps in Seeing*. Sinauer Associates, Sunderland.

- Roorda, A., Campbell, M. C. W. Atkinson, M. R. & Munger, R., 1997, in Vision Science and Its applications. Technical Digest Series, vol. 1, OSA, Wasington, DC, p. 90.
- Schnapf, J.L. & Baylor, D. A., 1987, *Sci. Am.* 256, 40.
- Smith, G. & Atchison, D. A., 1997, *The Eye and Visual Optical Instruments*. Cambridge Univerity Press, Cambridge.
- Wade, A. R. & Fitzke, F. W., 1998, *Lasers and Light* 8, 129.
- Walsh, G. & Charman, W. N., 1985, *Ophthalmic. Physiol. Opt.*, 5, 23.
- Wandell, B. A., 1995, *Foundations of Vision*. Sinauer Associates, Sunderland.
- Williams, D. R., MacLeod, D. I. A. & Hayhoe, M., 1981, *Vision Res.*, 21, 1357.
- Williams, D. R. & Collier, R. J., 1983, *Science*, 221, 385.
- Williams, D. R., 1985a, *Vision Res.*, 25, 195.
- Williams, D. R., 1985b, *J. Opt. Soc. Am. A*, 2, 1087.
- Williams, D. R., 1988, *Vision Res.*, 28, 433.
- Williams, D. R., Liang, J., Miller, D. T. & Roorda, A., 2000, in: *Adaptive Optics Engineering Handbook* (Ed. R. K. Tyson; cap. 10), Marcel Dekker, Inc., New York.